BENCH-SCALE TESTS OF A YUCCA MOUNTAIN HEATED DRIFT ENVIRONMENT

Prepared for

U.S. Nuclear Regulatory Commission
Contract NRC–02–07–006

Prepared by

T. Mintz
R. Pabalan
C. Manepally

Center for Nuclear Waste Regulatory Analyses
San Antonio, Texas

September 2011

ABSTRACT

The lifetime of a waste package emplaced in a potential repository can be estimated by evaluating the expected degradation modes and their corresponding degradation rates. The susceptibility of a material to a particular degradation mode and the severity of that degradation will depend upon the environment to which it is subjected. Key parameters of the environment include both the temperature and chemical constituents. The variation in these two quantities can significantly affect lifetime prediction of the component or structure. The evolution of this environment may be influenced by several factors including quantity and chemistry of the seepage water. In addition, temperature and relative humidity are environmental factors that will modify the degradation types and severity for a waste package placed in a potential repository drift. However, the difficulty in determining the actual environment is a challenge due to the heterogeneity of the natural system, interactions between the engineered and natural components, the unsaturated conditions at the repository horizon, the potential for natural drift degradation in a thermally perturbed environment, and evolution of the near-field environment.

To evaluate this complex system, in 2007 a scaled model of a drift environment for a potential repository was developed to estimate how heat in a drift may modify the environmental condition surrounding a waste package. The relationships between the evolution of the water chemistry as a function of temperature, infiltration flux, relative humidity, and corrosion rates were evaluated. The experimental setup consisted of a cuboid container filled with quartz sand. A stainless steel tube was placed in the middle of the container simulating the underground drift. The environmental conditions were monitored using corrosion and temperature sensors placed in the stainless steel mesh and in the surrounding porous media. These sensors allowed for the interpretation of the evolution of environmental conditions in the porous media. The only test that was conducted before the experiment was stopped consisted of allowing deionized water to percolate through the system during a 3-month test period. Solution was extracted from various regions in the experimental system and analyzed to understand the evolution of environmental conditions. The report discusses the experimental setup and the results, which initially indicate that there is a progressive change in the chemical activity and thermal conditions in the region surrounding the emplacement drift.

CONTENTS

Section Page

ABSTRACT ii
FIGURES iv
TABLE v
ACKNOWLEDGMENTS vi

1 INTRODUCTION 1-1

2 EXPERIMENTAL DETAILS 2-1
2.1 Experimental Setup 2-1
2.2 Experimental Procedure 2-5

3 RESULTS 3-1
3.1 Temperature Sensors 3-1
3.2 Corrosion Sensors 3-1
3.3 Chemical Analyses 3-7

4 DISCUSSION 4-1

5 CONCLUSIONS 5-1

6 REFERENCES 6-1

FIGURES

Figure		Page
1-1	Schematic Diagram of the Waste Package in Emplacement Drift	1-2
2-1	Scaled Model System Prior to Addition of Porous Quartz Media, Sensors, and Heaters	2-2
2-2	Scaled Model System Showing the Location of the Corrosion and Temperature Sensors	2-3
2-3	Corrosion Sensors Used to Estimate the Corrosivity of Local Environment	2-4
3-1	Temperature Sensor Profile During the Deionized Water Infiltration Test	3-2
3-2	Relative Current Values From Corrosion Sensors Placed 15 cm [6 in] Vertical of the Stainless Steel Mesh	3-3
3-3	Relative Current Values From Corrosion Sensors Placed 3 cm [1 in] Vertical of the Stainless Steel Mesh	3-4
3-4	Relative Current Values From Corrosion Sensors Placed in the Stainless Steel Mesh Structure	3-5
3-5	Relative Current Values From Corrosion Sensors Placed 8 cm [3 in] Horizontal of the Stainless Steel Mesh	3-6
3-6	Relative Current Values From Corrosion Sensors Placed 8 cm [3 in] Horizontal of the Stainless Steel Mesh (Expanded)	3-7

TABLE

Table Page

3-1 Solution Composition Analyses From Four Bottom Chambers 3-8

ACKNOWLEDGMENTS

This report describes work performed by the Center for Nuclear Waste Regulatory Analyses (CNWRA®) for the U.S. Nuclear Regulatory Commission (USNRC) under Contract No. NRC–02–07–006. The activities reported here were performed on behalf of the USNRC Office of Nuclear Material Safety and Safeguards, Division of High-Level Waste Repository Safety. This report is an independent product of CNWRA and does not necessarily reflect the view or regulatory position of USNRC.

The authors gratefully acknowledge X. He for her technical review, K. Axler for his programmatic review, L. Mulverhill for her editorial review, and A. Ramos for his administrative support. Special thanks to Mr. B. Derby for his assistance in conducting the experiments described in this study.

QUALITY OF DATA, ANALYSES, AND CODE DEVELOPMENT

DATA: All CNWRA-generated original data contained in this report meet the quality assurance requirements described in the Geosciences and Engineering Division Quality Assurance Manual. Sources for other data should be consulted for determining the level of quality for those data. All data and calculations related to this report have been recorded in CNWRA Scientific Notebook 768 (Dunn and Mintz, 2011).

ANALYSES AND CODES: No codes were used in the analyses of the work described in this report.

Reference

Dunn, D. and T.S. Mintz. "Integrated Tests—Initial Testing." Scientific Notebook No. 768. San Antonio, Texas: Center for Nuclear Waste Regulatory Analyses. pp. 55–89. 2011.

1 INTRODUCTION

Nuclear waste disposal packages are currently used and are potentially going to be used in many disposal applications. Some potential deep geological disposal sites include the Finnish repository that has proposed using buffer and backfill and the potential Japanese repository that is considering a similar concept (NEA, 2004). In addition, the U.S. Department of Energy (DOE) proposed to dispose nuclear waste at Yucca Mountain using a waste package consisting of an outer layer manufactured from Alloy 22, as seen in Figure 1-1.

To predict the lifetime of the waste canister material used in a potential repository, it is essential to understand the potential types and rates of degradation that could occur in the emplacement drift. Most forms of degradation are affected by environmental conditions. Localized corrosion, which can be in the form of crevice corrosion or pitting, is affected by both temperature and the chemical environment (Pardo, et al., 2000). For example, crevice corrosion on Alloy 22 in proposed Yucca Mountain repository conditions was shown to be a function of the exposure conditions (Dunn, et al., 2005). Another form of localized corrosion that may affect underground structures is stress corrosion cracking. Stress corrosion cracking susceptibility was also shown to be a function of environmental exposure conditions for Alloy 22 (Chiang, et al., 2005).

The types and rates of degradation can be measured in a laboratory setting; however, one must first know the environmental exposure conditions that the waste package could experience. Several environmental factors are important to lifetime calculations, including temperature, quantity and chemistry of seepage water, and relative humidity. The primary factor affecting temperature and relative humidity inside a drift is heat load in the postclosure period. The evolution of the surrounding environment is a complex process due to the heterogeneity of the natural system. Surrounding porous media properties may affect the fluid flow regime, pore water chemistry, and relative humidity, which in turn, will affect corrosion rates. Depending on the chemical constituents of the surrounding porous media, the solution that may reach the waste package could potentially range from acidic to basic. Two key features in porous media that may affect the corrosion severity of the drift environment are the amount and type of soluble salts and the moisture content. Understanding the evolution of these environmental conditions is necessary in gaining a perspective on the initiation and propagation of various degradation modes for an underground structure.

The subject research described in this report is the second phase in an approach to estimate the composition of the salts that form during the thermal period that would potentially occur in a repository. This system was not used to simulate an exact condition in a repository, but provide a simple setup to start identifying key parameters that must be understood. The first phase of this project was conducted in 2006 and examined the effect of dripping solutions onto a heated Alloy 22 sample. In this phase, an Alloy 22 sample was heated to roughly 115 °C [239 °F]. Different types of pore water solutions were allowed to drip onto the surface of the heated Alloy 22 sample. The composition and properties of the salts and solutions that formed on the heated Alloy 22 surface were measured. The results of this test, described in Dunn, et al.

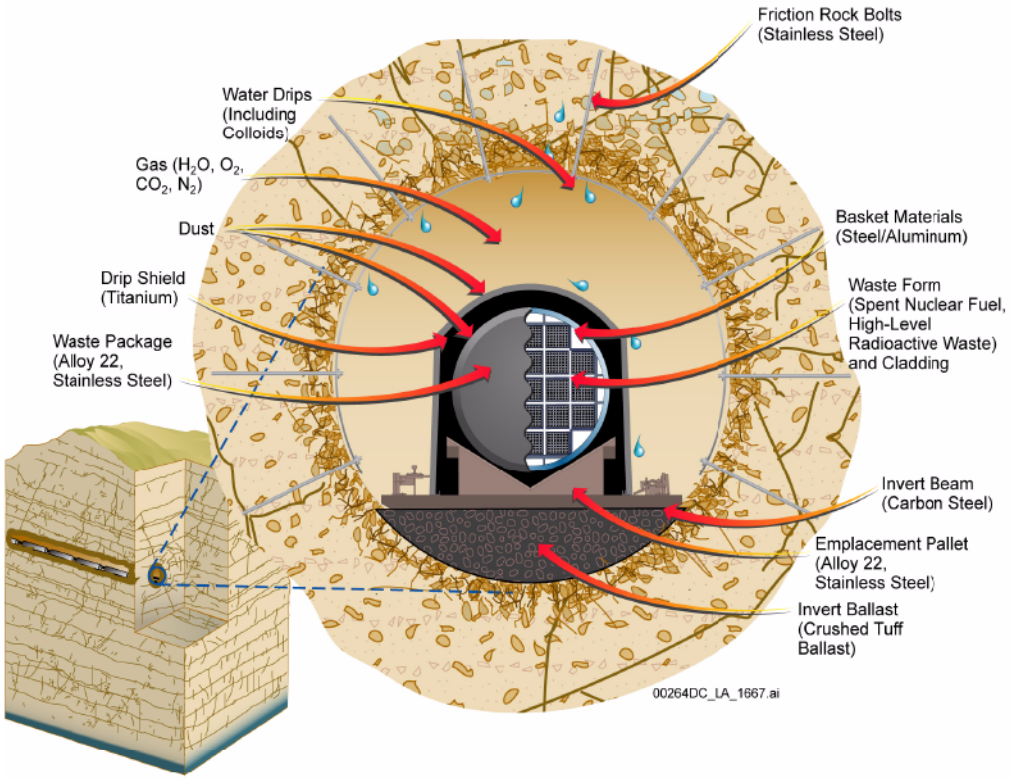

Figure 1-1. Schematic Diagram of the Waste Package in Emplacement Drift (DOE, 2008)

(2006), showed that the final salt deposit depended on the initial composition of the dripping solution. The results also indicated that deliquescent salt deposits or brines were not likely to form under the tested conditions. The following phase of this testing was conducted in 2007 and is described in the remaining sections of this report.

2 EXPERIMENTAL DETAILS

2.1 Experimental Setup

A scaled model of an underground drift was developed to replicate the surrounding environmental conditions a waste package may experience. The experimental setup consisted of a polycarbonate cuboid container, as shown in Figure 2-1. The container was filled with quartz sand as the porous media because it is chemically inert and should minimize any modification of the water chemistry that is introduced to the scaled model system. In subsequent tests, which did not occur, the quartz sand was to be replaced with media more closely related to those found at Yucca Mountain. The polycarbonate container was 122 cm [48 in] high, 50 cm [20 in] wide, and 50 cm [20 in] deep. A hollow stainless steel mesh tube was placed in the middle of the container simulating the emplacement drift. The stainless steel mesh restrained the porous quartz media while allowing liquid to penetrate the mesh. The key attribute of the test system design is the dimensions, which provide sufficient height so that liquid flow through the system can be influenced by the heat source within the stainless steel structure.

The temperature of the system was controlled using two sources of heat, as shown in Figure 2-2. There was an internal heater centered inside the stainless steel mesh structure. This internal heater simulated a heat source in the emplacement drip from a waste package. In addition to the central heater, there were heaters located around the exterior of the system and covered by insulation. The exterior heaters maintained a constant temperature gradient from the central heater and the outer walls of the experimental system. This gradient removed any cold spots where the water could condense on the outer walls and flow straight into the bottom of the unit. There were no heaters on the top or bottom of the scaled model. All the heaters were powered by controllers and temperature feedback to allow for better control of the system temperature.

To monitor the evolution of environmental conditions in the porous media, corrosion and temperature sensors were placed at specific positions in the scaled model, as shown in Figure 2-2. The corrosion sensor consisted of a dissimilar metal coupling that could be a combination of either Alloy 22/A516 Grade 60 carbon steel or Alloy 22/Type 304 stainless steel. Each type of corrosion sensor was placed at four locations. The two types of corrosion sensors were placed in the stainless steel mesh (i) 3 cm [1 in] above the stainless steel mesh, (ii) 15 cm [6 in] vertical of the stainless steel mesh, and (iii) 8 cm [3 in] horizontal of the stainless steel mesh. The two types of corrosion sensors were separated in the depth direction of the scaled model by roughly 30 cm [1 ft] at each of the four locations. Each sensor was approximately 2.54 × 1.27 × 0.318 cm [1 × 0.5 × 0.125 in], as shown in Figure 2-3. The Alloy 22 samples had two 0.64-cm [0.25-in] holes drilled into them, as shown in Figure 2-3. The A516 carbon steel and Type 304 stainless steel were isolated from the Alloy 22 by a film of polyimide film (Kapton® Tape). Two areas were not covered by the polyimide film: (i) two holes on the A516 carbon steel or 304 stainless steel material that matched up with the holes on Alloy 22 And (ii) the area on the top of the sensor, which allowed moisture to reach both

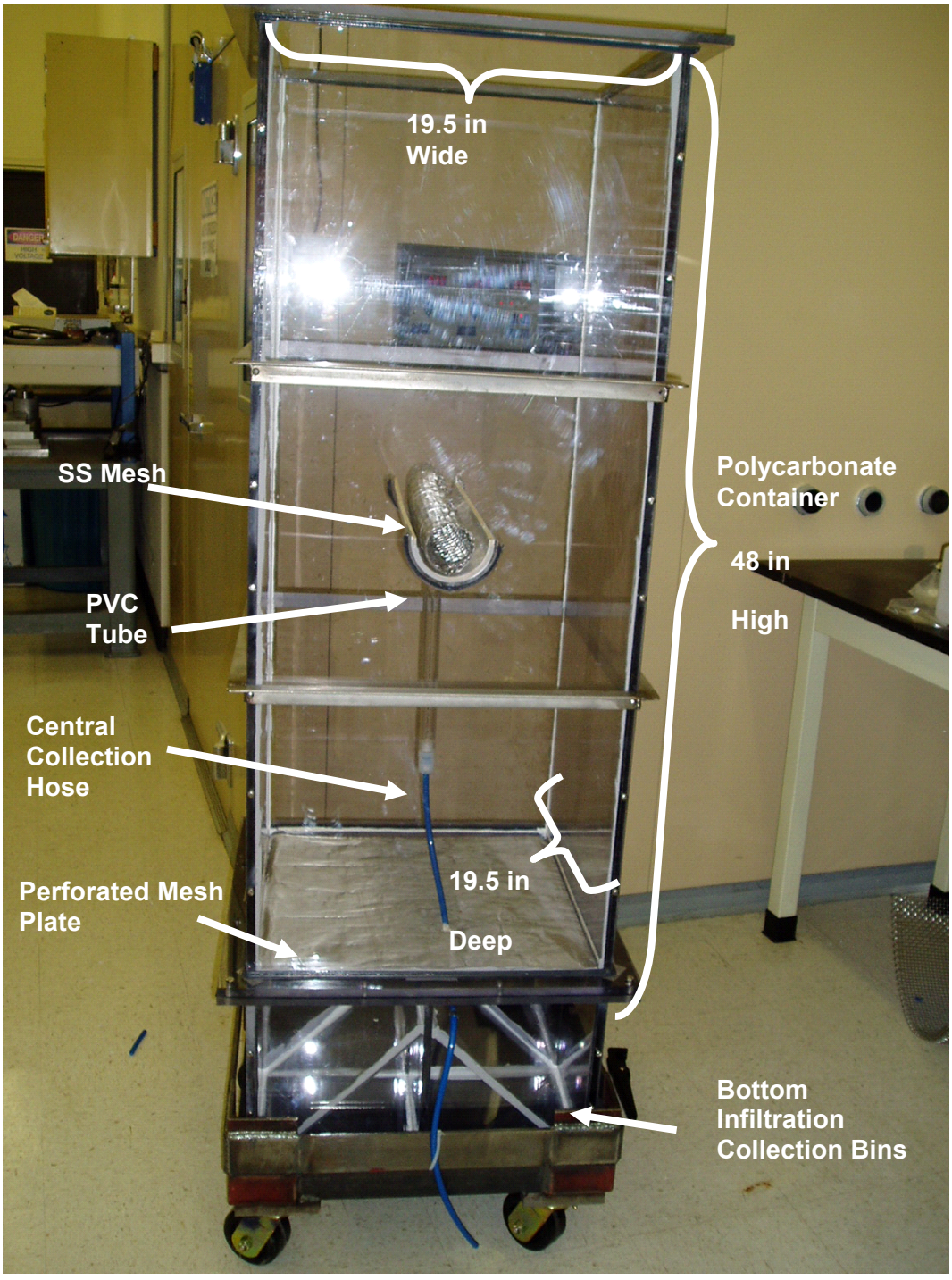

Figure 2-1. Scaled Model System Prior to Addition of Porous Quartz Media, Sensors, and Heaters.
Note: SS = Stainless Steel, PVC = Polyvinyl Chloride.

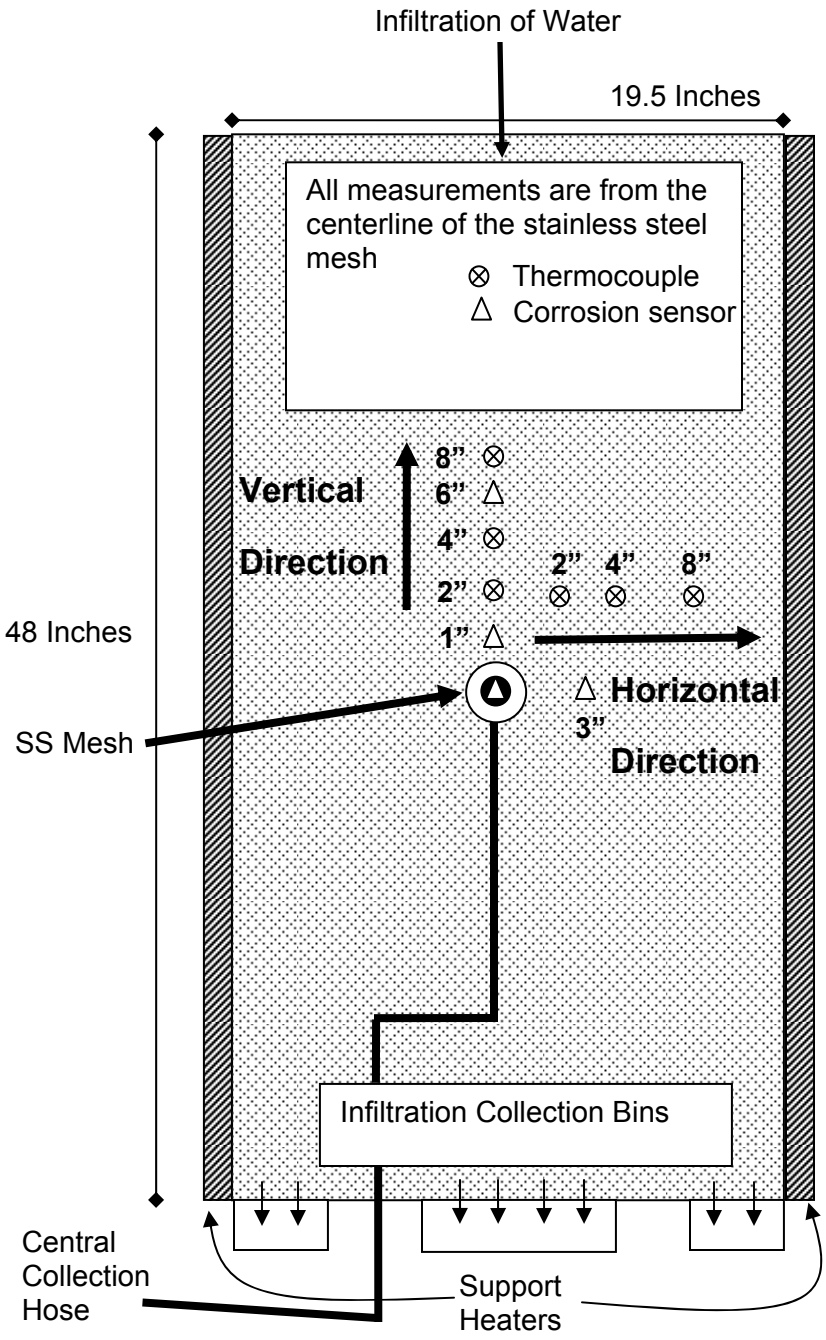

Figure 2-2. Scaled Model System Showing the Location of the Corrosion and Temperature Sensors. Distances Shown Are With Respect to the Center of the Stainless Steel Central Structure.
Note: SS = Stainless Steel.

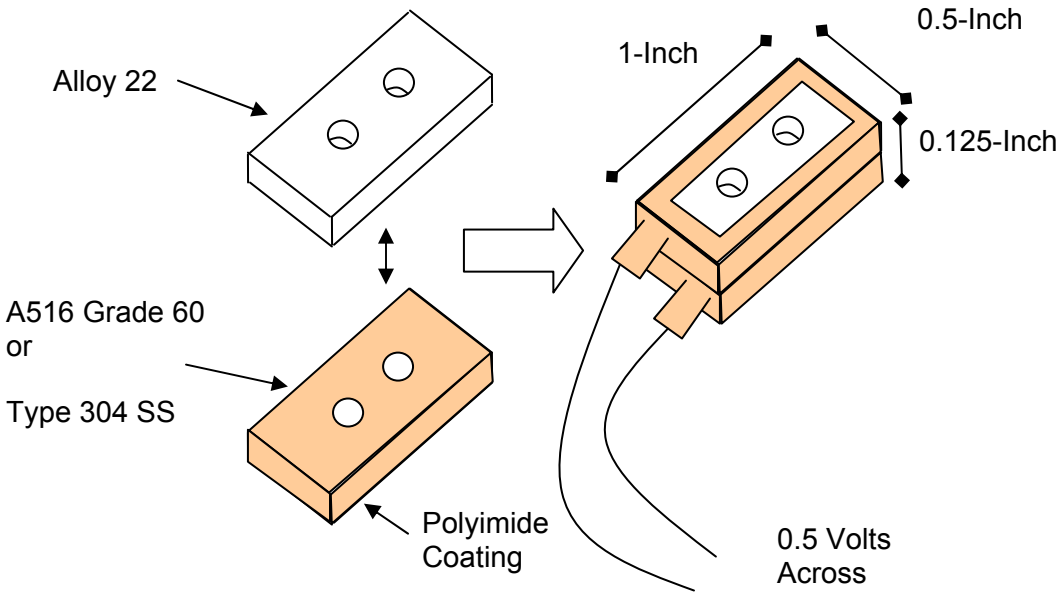

Figure 2-3. Corrosion Sensors Used to Estimate the Corrosivity of Local Environment

materials. However, both materials were electrically isolated from each other. After placing the two materials together, the system was wrapped in the same polyimide film as shown in Figure 2-3. During the test, the sensors were held at a biased voltage of 0.5 volts with the A516 carbon steel or Type 304 stainless steel as the anode and the Alloy C22 as the cathode. If liquid accumulated in the Alloy 22 holes, this accumulation would be sensed by a change in the measured current. In addition, the sensor response should be consistent with the corrosivity of the accumulated moisture.

Each corrosion sensor location, as shown in Figure 2-2, consisted of the two types of sensors. These two corrosion sensors were separated in the depth direction by roughly 30 cm [12 in]. The two types of corrosion sensors provided different sensitivities to the corrosivity. The Alloy 22/A516 carbon steel sensor provided a much larger current, whereas the Alloy 22/304 stainless steel corrosion sensor provided a more sensitive measurement. The difference in sensitivities is due to the difference in the galvanic interactions. There is a much larger difference in the electrode potentials between the Alloy 22 and A516 carbon steel than between the Alloy 22 and the Type 304 stainless steel. Therefore, because there is a larger driving force on the Alloy22/A516 carbon steel sensor, if the same solution electrically connects these two materials, there will be a much larger resulting current for this sensor than for the Alloy 22/304 stainless steel sensor.

In addition to the corrosion sensors, the model system was implemented with six temperature sensors, as shown in Figure 2-2. Three of the temperature sensors are located vertically above the stainless steel mesh structure, while the other three are located horizontal of the stainless steel mesh structure. The distances vertically and horizontally from the stainless steel central structure were the same at 5, 10, and 20 cm [2, 4, and 8 in]. These temperature sensors were initially recorded manually; however, it was determined that more frequent measurements were

needed, and the temperature recording was automated with computerized data acquisition during the experiment.

Water chemistry was measured from two different areas. One area was at the bottom of the scaled model system. As illustrated in Figures 2-1 and 2-2, there are collection bins on the bottom of the scaled model system. The collection bins were separated from the quartz media by a perforated mesh plate. The plate allowed the liquid to pass through while holding the quartz sand in place. Liquid that percolates through the quartz sand that does not reach the center stainless steel mesh structure was collected in these bottom infiltration chambers. Any liquid that reaches the center stainless steel structure will collect in the bottom of the stainless steel mesh, where there is a polyvinyl chloride tube that has been bifurcated down the axial length. A hose attached to the bottom of the bifurcated polyvinyl chloride tube collects the water that reaches the stainless steel structure.

By measuring the temperature, moisture, and chemical content from various points in this system, one can gain an understanding of the relationship between the starting drip water and evolution of the water chemistry as a function of temperature and time.

2.2 Experimental Procedure

The scaled model was initially dried out after adding the quartz sand and installing all of the corrosion and temperature sensors. The scaled model dry out was conducted by raising the outer support heaters to 80 °C [176 °F] and holding the system at that temperature for 3 months. After the dry out was complete, an initial test of the system was performed using deionized water to establish base-line performance of the scaled system. The infiltration rate of the deionized water was set at 1 L/day [0.264 gal/day] as a point source directly in the center of the top surface of the quartz sand, shown in Figure 2-2. The top of the test system was covered and insulated to reduce the escape of water due to evaporation. The experimental setup was located in an environmental chamber that reduced the ambient external temperature and relative humidity variations caused by diurnal and seasonal changes by controlling these properties roughly between 60 and 70 percent relative humidity and 23 and 25 °C [75 and 76 °F]. The internal central heater was held at 110 °C [230 °F], which provided a temperature gradient of 30 °C [54 °F] between the outer walls and underground structure. The corrosion sensor currents were measured using a data acquisition system. The temperature measurements were initially measured manually, and after 60 days of testing, they were measured by a data acquisition system. The overall duration of the test was approximately 3 months. The collected solutions were analyzed for chemical composition.

3 RESULTS

The following sections describe the results of the deionized water infiltration testing analysis. The interpretation of the temperature sensor data, corrosion sensor data, and chemical analysis indicates how the water content in the system evolved over time.

3.1 Temperature Sensors

There were six temperature sensors placed into the surrounding quartz porous media. These sensors showed the change in temperature, which is affected by the evolution of the thermal conductivity of the porous media. The change in the thermal conductivity is a result of the evolution of the moisture level throughout the porous media. The temperature profiles for all six sensors over the period of the test are shown in Figure 3-1. Day 0 is when the infiltration of deionized water started. The conductive heat transfer process dictates the temperature distribution in the surrounding porous media. This effective conductivity in the porous media is dependent on the degree of liquid saturation in the media that is dependent on the infiltration rate of the deionized water. Convective heat transfer dominates in the air gap between the central heater and the stainless steel mesh wall. This explains the significant temperature difference between the central heat source set point temperature and the temperature sensor located at 5 cm [2 in]. Higher temperatures were observed at the temperature probes closest to the stainless steel structure. As can be seen in Figure 3-1, there was a larger temperature gradient in the vertical direction than in the horizontal direction. This is attributed to the support heaters laterally surrounding the test system. The top boundary of the experimental setup was open to external ambient temperature {approximately 27 °C [81 °F]} and resulted in a higher temperature gradient in the vertical direction compared to the lateral direction. This resulted in a lower temperature at the sensor located 20 cm [8 in] vertically above the central heater compared to the sensor located 20 cm [8 in] horizontally from the central heater. However, even in the horizontal direction, the temperatures were warmer toward the central heater, as would be expected. Once the test was initiated, all of the temperature sensors equilibrated to the new moisture level in the surrounding porous media. The 20-cm [8-in] vertical sensor, which was the coolest, showed an increase in temperature, while the other 5 hottest sensors showed a decrease in the temperature as moisture was added to the system.

3.2 Corrosion Sensors

Eight corrosion sensors were placed in the test system as shown in Figure 2-2. Figures 3-2 through 3-6 indicate the relative change in currents from the moisture addition to the test system. The relative current was calculated by taking the base current value at Day 0 and then subtracting this from all of the following data measurements. The base current for each corrosion sensor ranged from −10 μA to −50 μA. Note that in Figure 3-3, the Alloy 22/304 stainless steel sensor data only goes to roughly 25 days because the sensor malfunctioned at that time.

Figure 3-2 shows the response of the corrosion sensors located 15 cm [6 in] above the central stainless steel mesh. Both sensors behave similarly in that there is an initial increase in the relative current that corresponds with the change in temperature observed in Figure 3-1. The maximum positive relative current observed for the Alloy 22/A516 carbon steel sensor was 0.75 μA, while the Alloy 22/304 stainless steel sensor reached a maximum relative current of

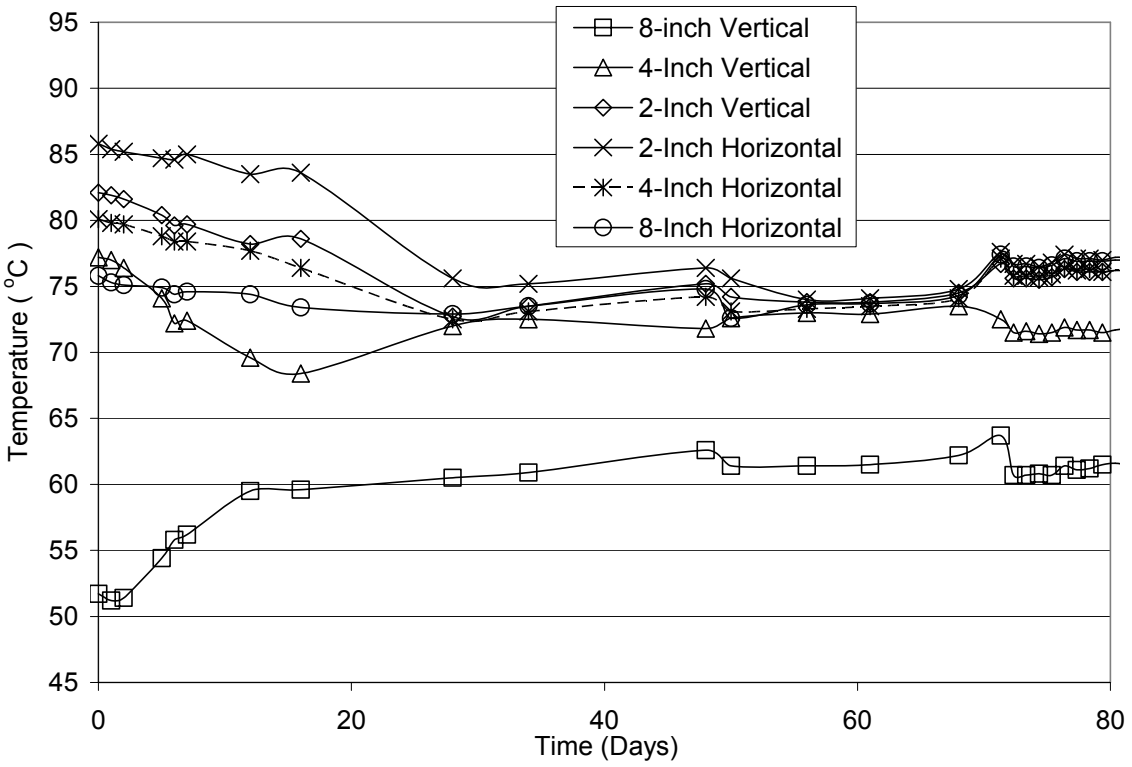

Figure 3-1. Temperature Sensor Profile During the Deionized Water Infiltration Test

roughly 0.5 μA. The relative current then started to slowly decrease for both corrosion sensors and finally ended up at a negative relative current value. The final equilibrium current value for the Alloy 22/A516 carbon steel sensor was roughly −0.10 μA, while the Alloy 22/304 stainless steel sensor equilibrated at −0.5 μA.

Figure 3-3 shows the relative current for the corrosion sensors located 3 cm [1 in] above the central stainless steel mesh. As mentioned previously, the Alloy 22/304 stainless steel corrosion sensor malfunctioned roughly 25 days into the test. However, the data indicate that both sensors saw an overall increase in the relative current with time. The Alloy 22/A516 carbon steel corrosion sensor reached an equilibrium relative current value of 1.5 μA at roughly 45 days into the test. This corrosion sensor indicated some spikes in the relative current, indicative of potential localized corrosion events. These spikes were on the order of only 1 μA. Secondly, there was a large trough in the relative current value for the Alloy 22/A516 carbon steel corrosion sensor, indicating either a relative dry period or a change toward a more benign chemistry.

Figure 3-4 presents the relative current values for the corrosion sensors that were located inside the central stainless steel mesh structure. The results of these data also indicate an increase in the relative current for both sensors. The Alloy 22/A516 carbon steel corrosion sensor reached a maximum relative current of roughly 6.5 μA at 70 days of testing. The Alloy 22/304 stainless steel corrosion sensor reached a maximum relative current value of 3 μA at roughly 10 days. There are no relative current spikes indicating any localized corrosion; however, these equilibrium relative currents are the largest observed by any of the corrosion sensors and are attributed to a more corrosive (concentrated) solution.

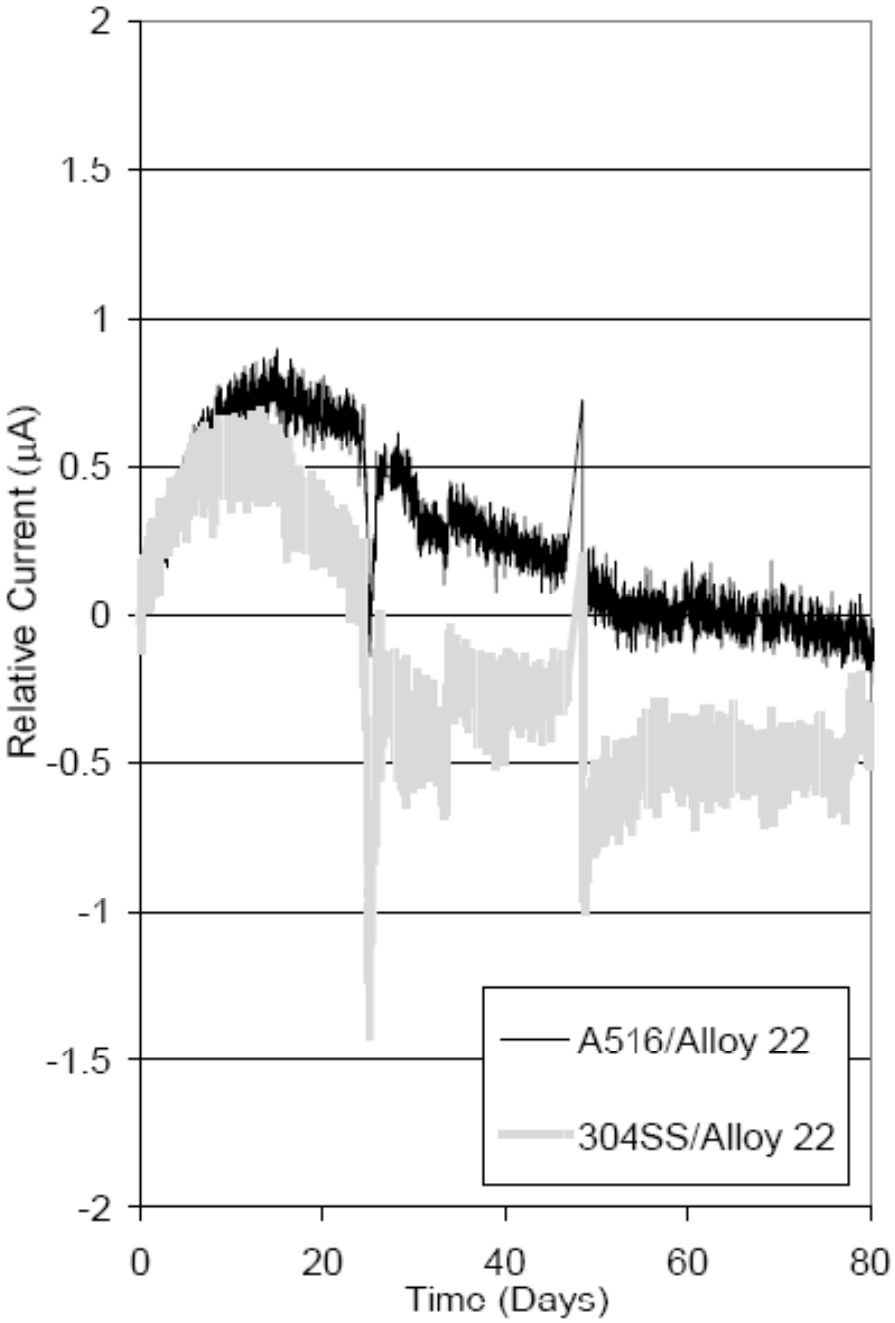

Figure 3-2. Relative Current Values From Corrosion Sensors Placed 15 cm [6 in] Vertical of the Stainless Steel Mesh

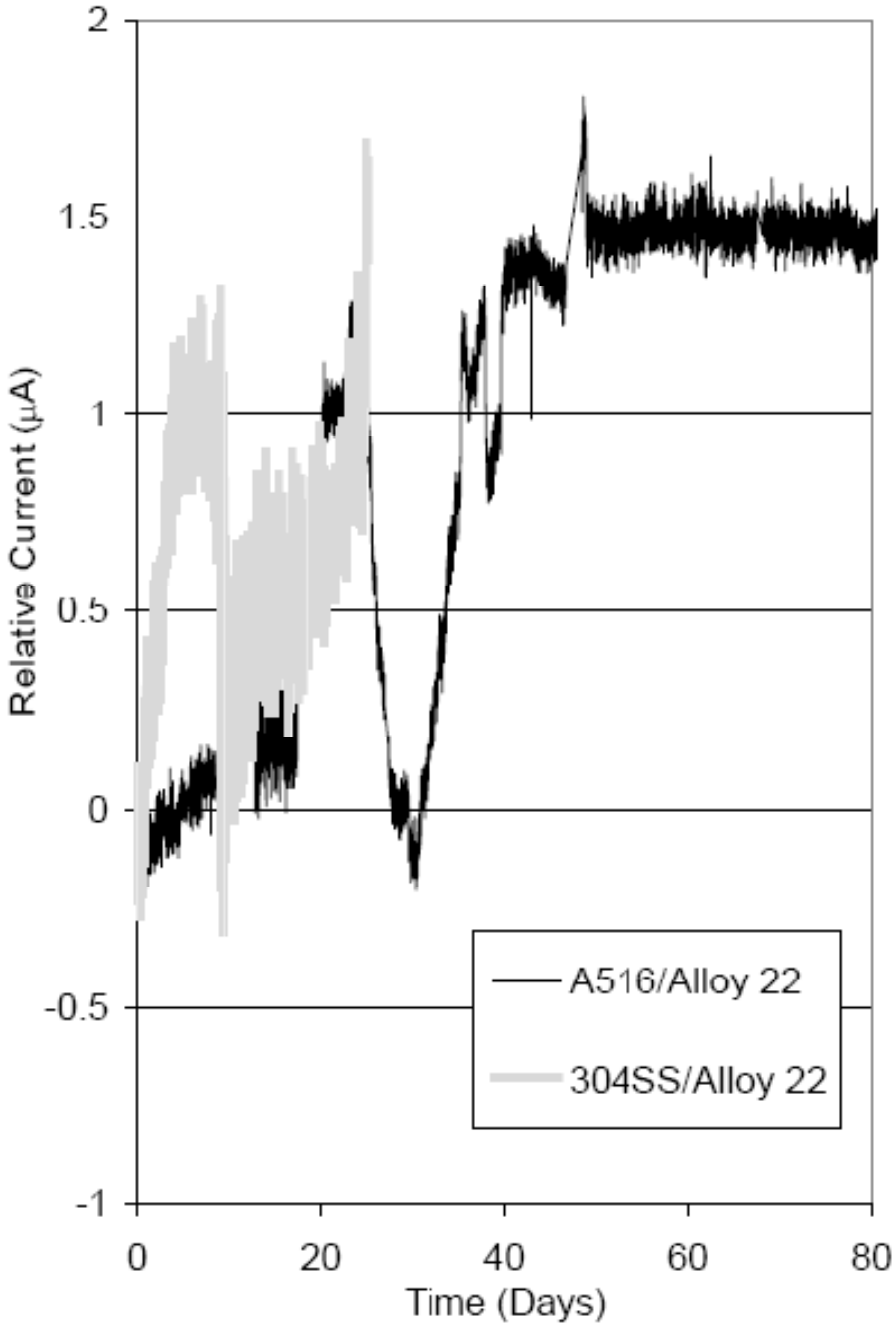

Figure 3-3. Relative Current Values From Corrosion Sensors Placed 3 cm [1in] Vertical of the Stainless Steel Mesh

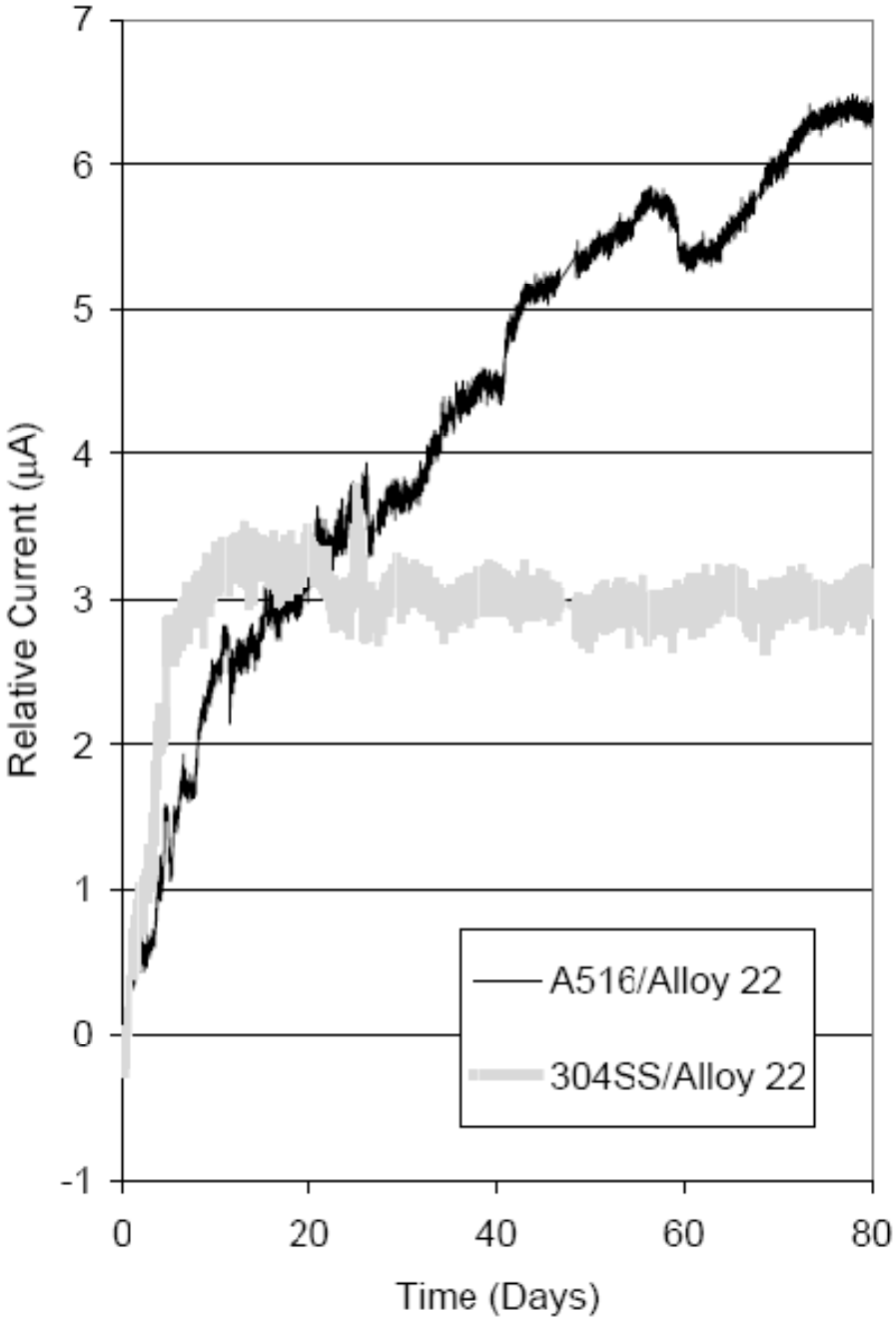

Figure 3-4. Relative Current Values From Corrosion Sensors Placed in the Stainless Steel Mesh Structure

Finally, Figures 3-5 and 3-6 show the relative current values for the corrosion sensors placed 8 cm [3 in] horizontally from the central stainless steel mesh structure. As can be seen in Figure 3-5, there is a large relative current spike for the Alloy 22/A516 carbon steel corrosion sensor to roughly −425 μA. It is unclear whether this indicates a change in the corrosivity at this sensor or an electronic error in the sensor. A closer image of the current values relative to base-line is provided in Figure 3-6. As can be observed in the figure, the current behaved similarly to the corrosion sensors placed 15 cm [6 in] vertical of the stainless steel mesh as

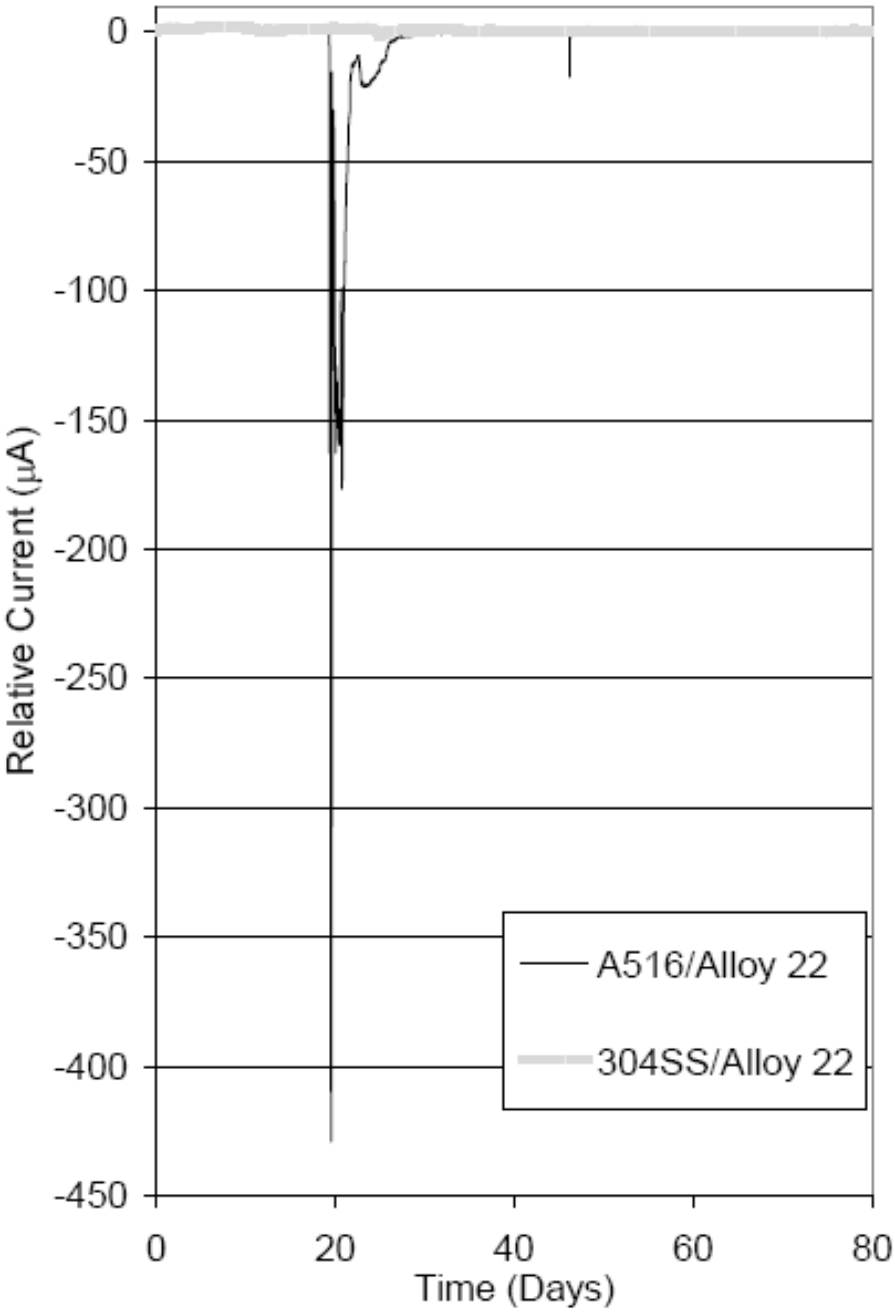

Figure 3-5. Relative Current Values From Corrosion Sensors Placed 8 cm [3 in] Horizontal of the Stainless Steel Mesh

shown in Figure 3-2. The relative current initially increased and then decreased. The maximum relative current was roughly 2.2 μA and 2 μA for the Alloy 22/A516 carbon steel corrosion and Alloy 22/304 stainless steel corrosion sensors, respectively. The final equilibrium relative current for both corrosion sensors was roughly −0.3 μA and 0.3 μA for the Alloy 22/A516 carbon steel and Alloy 22/304 stainless steel corrosion sensors, respectively.

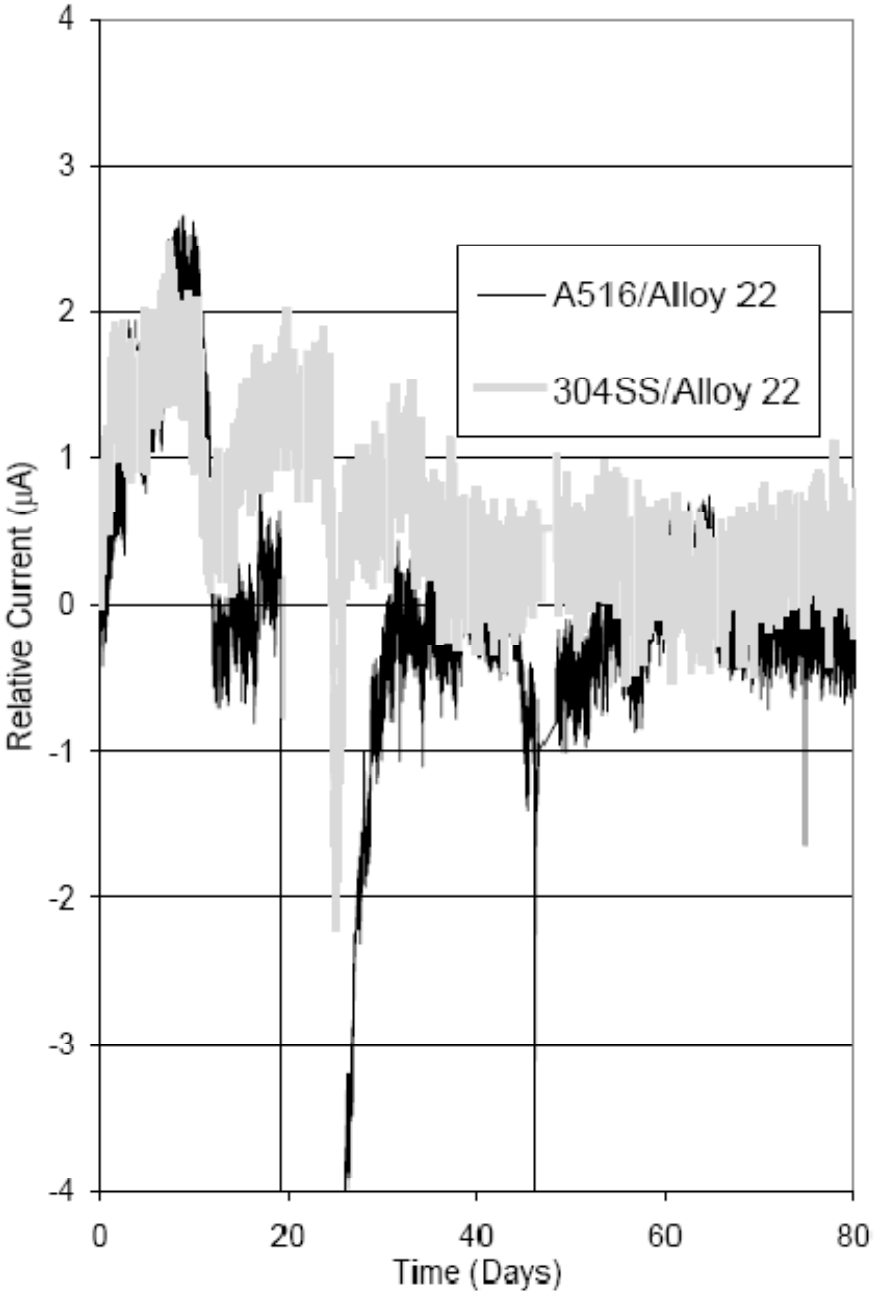

Figure 3-6. Relative Current Values From Corrosion Sensors Placed 8 cm [3 in] Horizontal of the Stainless Steel Mesh (Expanded)

3.3 Chemical Analyses

As previously mentioned, solution was collected from both the bottom of the testing system and the central stainless steel mesh structure. The bottom infiltration collection bins were separated

into four different chambers. The liquid in each chamber was collected and chemically analyzed. The composition of the liquid in each of these four chambers and the results of the liquid collected from the stainless steel structure are shown in Table 3-1. The liquid analyzed was from the total accumulated liquid collected during the whole test.

As can be seen from Table 3-1, the liquid collected at the bottom of the test system is mostly uniform in composition. From the data presented in Table 3-1, it appears that leaching did occur from the quartz sand as deionized water passed through the system. However, it is the differences between the liquid that was collected in the bottom chambers and that collected from the stainless steel central structure that is of interest. While the concentration of silicon from the bottom chamber 1 was much higher, the concentration of boron, calcium, sodium, and sulfur were very similar in all the bottom chambers. Comparing the bottom chambers to the values collected from the central stainless steel structure was quite different. There was a much higher level of sulfur, sodium, boron, and phosphorus in the liquid collected from the stainless steel central structure. This increased concentration in the central stainless steel structure is likely due to the higher temperatures, which may have let to evaporation and a concentrating effect.

Table 3-1. Solution Composition Analyses From Four Bottom Chambers*

Locations	Boron (mg/L)	Calcium (mg/L)	Silicon (mg/L)	Sodium (mg/L)	Sulfur (mg/L)	Phosphorus (mg/L)
Bottom Chamber 1	4.91	8.25	54.4	6.32	1.72	<0.200
Bottom Chamber 2	5.18	1.64	16.1	5.97	<1.00	<0.200
Bottom Chamber 3	2.07	1.64	14.3	3.14	1.03	<0.200
Bottom Chamber 4	5.18	2.39	18.0	6.43	<1.00	<0.200
Stainless Steel Mesh	25.2	<1.25	17.8	38.7	108	1.21

*Solutions were analyzed for additional chemical species other than those listed. Only the species listed had reportable results.

4 DISCUSSION

The corrosion performance of a waste package emplaced in a drift environment will be dependent upon the surrounding porous media conditions. Underground metallic structures in a porous media environment can suffer from general corrosion, stress corrosion cracking, and localized corrosion (pitting or crevice). Changes in pH, moisture, temperature, and chemical content will affect the corrosion resistance of an underground metallic structure or system.

A scaled model of a heated emplacement drift was designed to examine how interactions with the surrounding porous media may affect the local environmental conditions. In the current scaled model, the inner stainless steel structure had a thermal heater held at 110 °C [230 °F]; however, the outer walls of this stainless steel structure were somewhere below this value. The outer walls of the scaled model were held at 80 °C [176 °F] by support heaters, while the top and bottom of the scaled model was in equilibrium with the room temperature air.

For the initial test, deionized water was added to the top of the system and allowed to equilibrate over a period of 3 months. Measurements were made from temperature sensors and corrosion sensors located in the test chamber. In addition, solution was collected from bins at the bottom of the test system and from the underground structure region and chemically analyzed.

The results of the temperature profile over the testing period showed that the temperatures changed quickly (roughly 10 days) and then slowly reached equilibrium at 25–30 days of the test. These results correspond to the peak relative current observed in both the vertical 15-cm [6-in] and horizontal 8-cm [3-in] corrosion sensors. Depending on the initial temperature at a particular sensor location, the temperature either increased or decreased with time. This difference in temperature was due to the different temperature gradients in the vertical and horizontal direction. Different gradients occurred because the support heaters on the lateral walls were held at 80 °C [176 °F], while the top of the system was held in equilibrium with the room temperature of 27 °C [81 °F]. However, the results indicate that the temperature of the media surrounding the stainless steel structure decreased as moisture was added to the system. While the decreased temperature may lead to less severe corrosion, the added liquid can lead to higher porous media conductivity and more corrosive solution, which can lead to higher corrosion rates.

The corrosion sensors, which indicate corrosivity, were placed in and around the stainless steel structure. The corrosion sensors that were 15 cm [6 in] vertically and 8 cm [3 in] horizontally away from the stainless steel structure showed an initial increase in the relative current that could be taken as an increase in moisture and, as such, corrosivity. However, the relative current decreased roughly 10 days after the infiltration was initiated. The results suggest that the environmental conditions in the outer porous media reached equilibrium quickly. This is based on the initial relative current increase observed for the corrosion sensors. Once the equilibrium condition had been obtained, an oxide film likely continued to build on the materials, leading to the lower relative currents observed for the corrosion sensors.

Both the 2.5-cm [1-in] corrosion sensors and corrosion sensors in the central stainless steel structure showed an increase in the relative current to a much higher degree. This indicates a much more corrosive environment, which is consistent with the results from the chemical analysis showing a much more concentrated solution at the central stainless steel structure. The additional time needed to reach an equilibrium relative current value for the corrosion sensors at 2.5 cm [1 in] and in the stainless steel mesh structure is thought to be related to the

evaporation and a concentrating effect. Because of the higher temperatures at the stainless steel mesh structure, it will take a longer time to reach an equilibrium condition. However, the Alloy 22/304 stainless steel sample does not take long to reach equilibrium, because it builds up a chromium oxide film inhibiting further degradation.

The chemical analysis examined the variation of the chemistry in the surrounding porous quartz media compared to the chemistry of liquid around the central stainless steel structure. The quartz sand should have been composed only of silicon-oxygen tetrahedra particles and inert. However, the quartz must have contained other constituents, which was dissolved into the deionized water. Therefore, the original assumption that the quartz would be inert was incorrect. The results indicate that there was a difference in the chemistry surrounding a stainless steel structure versus the solution that was collected at the bottom of the scaled model. In this case, there was a large increase in the concentration of sulfur in the liquid near the stainless structure. Sulfur is a chemical element that has been known to accelerate corrosion in various materials (Ahn, et al., 2008; Yang, et al., 2004). Therefore, observed changes in chemistry explain the higher corrosion rate for the corrosion sensor located closed to the central heated structure. Note that even though quartz sand was used and was expected to be inert, there was an interaction between the porous media and dripping deionized water.

5 CONCLUSIONS

Waste canisters that are being considered for use in underground repositories of high-level radioactive waste and spent nuclear fuel are susceptible to various forms of degradation. The severity of these degradation modes is dependent upon the local environment. The evolution of the environment in the near field is a complex process due to the heterogeneity of the natural system. The subject research described in this report is the second phase of an approach to estimate the composition of the salts that form on a waste package in a proposed repository drift during the thermal period. This first phase, conducted in 2006, examined the salt composition that would form when repository ground water was dripped onto the surface of heated Alloy 22 material. This second phase, conducted in 2007, examined the chemical changes of an aqueous solution as it moves through heated porous matrix.

A scaled model of an underground drift was developed to mimic the surrounding environmental conditions that a waste package may experience. Temperature and corrosion sensors were placed in this scaled model to characterize the evolution of the environmental conditions as solution was allowed to percolate through the system. The first test consisted of deionized water dripping directly in the center of the top surface of the quartz sand that was used to fill the scaled model. The pseudo-drift temperature was maintained at 110 °C [230 °F], while the walls of the scaled model were kept at 80 °C [176 °F] (not including the top and bottom of the scaled model). This control test was used to observe how the scaled model behaves. This was the only test conducted, because the experimental work was put on hold after completing this initial control test.

The results of the deionized water test in the scaled model indicate that the porous media on the walls of an emplacement drift will differ in moisture level, temperature, and chemical species from the main porous matrix during the thermal period. The composition of the solution that reached the pseudo-emplacement drift in the scaled model was concentrated in boron, sodium, phosphorus, and sulfur compared to solution that percolated through the system. The corrosion sensors indicated that the concentrated environment at the pseudo-drift was much more corrosive than the environment farther from the internal heater.

6 REFERENCES

Ahn, T., H. Jung, X. He, and O. Pensado. "Understanding Long-Term Corrosion of Alloy 22 Container in the Potential Yucca Mountain Repository for High-Level Nuclear Waste Disposal." *Journal of Nuclear Materials*. Vol. 379. pp. 33–41. 2008.

Chiang, K.T., D.S. Dunn, and G.A. Cragnolino. "Effect of Simulated Groundwater Chemistry on Stress Corrosion Cracking of Alloy 22." Proceedings of the CORROSION 2005 Conference. Paper No. 05463. Houston, Texas: NACE International. 2005.

DOE. DOE/RW-0573, "Yucca Mountain Repository License Application." Rev. 0. Las Vegas, Nevada: U.S. Department of Energy. 2008.

Dunn, D., Y.-M. Pan, X. He, L.T. Yang, and R.T. Pabalan. "Evolution of Chemistry and Its Effects on the Corrosion of Engineered Barrier Materials." 30th Symposium on the Scientific Basis for Nuclear Waste Management. Boston, Massachusetts: Material Research Society. 2006.

Dunn, D., O. Pensado, Y.-M. Pan, R.T. Pabalan, L.T. Yang, X. He, and K.T. Chiang. "Passive and Localized Corrosion of Alloy 22—Modeling and Experiments" CNWRA 2005-02. Rev. 1. San Antonio, Texas: Center for Nuclear Waste Regulatory Analyses. 2005.

NEA. Organization for Economic Co-Operation and Development. "Engineered Barrier Systems (EBS): Design Requirements and Constraints." ISBN 92-64-02068-3. Paris, France: OECD Nuclear Energy Agency. 2004.

Pardo, A., E. Otero, M.C. Merino, M.D. López, M.V. Utrilla, and F. Moreno. "Influence of pH and Chloride Concentration on the Pitting and Crevice Corrosion Behavior of High-Alloy Stainless Steels." *Corrosion*. Vol. 56, No. 5. pp. 411–418. 2000.

Yang, L. and G. Cragnolino. "Studies on the Corrosion Behavior of Stainless Steels in Chloride Solutions in the Presence of Sulfate Reducing Bacteria." CORROSION/2004. Paper No. 04598. Houston, Texas: NACE International. 2004.